Excerpt from the Proceedings of the 2011 COMSOL Conference in Stuttgart

Ability of Single-Well Injection-Withdrawal Experiments to Estimate Ground Water Velocity

F. Maier*[,1], K. Hebig[2],
Y. Jin[1] and E. Holzbecher[1]
[1]University of Göttingen, Geosience Center, Applied Geology
[2] Technical University Berlin, Applied Geosciences
*Corresponding author: 37077 Göttingen, Goldschmidstr. 3, fmaier@gwdg.de

Abstract: In this study we present a closer look on the single-well injection-withdrawal experiment (SWIW) also known as push-pull experiment and its ability to determine the groundwater velocity, as one of the major parameters concerning reservoir management and underground reservoir characterization. The model region used in this study consists of a circular 2D horizontal plane with a borehole cut out. The flow field is modeled using analytic and numerical solutions. Different modes like Darcy´s law, solute transport and partial differential equation are applied. A challenge in the model setup is the boundary change from Dirichlet BC to Neumann BC within the proceeding time-dependent study. Finally we present type-curves for different experiment scenarios. It is shown that these curves strongly depend on interaction between the parameters for groundwater velocity, pumping rates and the duration of the quiescence phase as well as the reservoir geometry, effective porosity and dispersivity.

Keywords: push-pull-experiment, SWIW, groundwater velocity, tracer, boundary condition change

1. Introduction

Subsurface reservoirs are currently used not only for mining, but also for fluid and /or heat storage or withdrawal. Tracer tests are a powerful tool to determine reservoir parameters. A tracer is a substance or parameter with known physical and chemical properties, e.g. dye, heat, radioactive isotopes etc.. In general the tracer is injected into the reservoir, left there for a while interacting with the reservoir and finally pumped back (Figure 1). There are several ways of performing a tracer test. In this study we present a closer look on the single-well injection-withdrawal experiment (SWIW) also known as push-pull experiment and its ability to determine the groundwater velocity, as one of the major parameters concerning reservoir management. The experiment design used in this study follows a suggestion from Leap and Kaplan (1988), whos experiment takes higher groundwater flow velocities into account.
In this study we discuss different modeling approaches, the analytical and numerical flow field solution and the parameter sensitivity of the experiment. In the last section we apply the results to interpret field data.

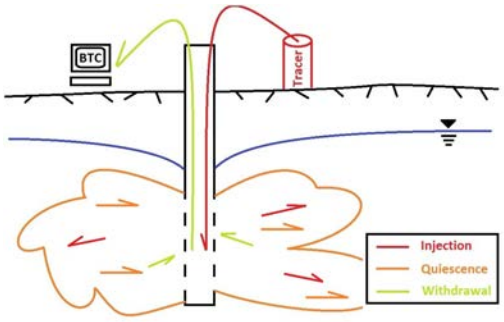

Figure 1: *Sketch of a SWIW tracer experiment. The colored arrows indicate the flow direction of the tracer.*

2. Objective

The reference model of this study is a SWIW experiment performed recently in Japan, in cooperation with Technical University Berlin. The experimental constraints were:

Table 1: Experimental constraints

Injection	247 min
Quiescence	1124 min
Pumping	1629 min
Injection rate	30 l min^{-1}
Pumping rate	16.79 l min^{-1}

In addition further reservoir constraints are known:

Table 2: Reservoir constraints form additional experiments

Aquifer thickness	10 m
Effective porosity	0.3
Hydraulic conductivity	$5 \cdot 10^{-6}$ m s^{-1}

3. Use of COMSOL Multiphysics

Comsol Multiphysics is used to compare the numerical flow field solution to the analytical solution, as well as the use of different modes to model the experiment. As a starting point we use the timescale, boundary conditions and initial conditions from filed data (Tables 1 & 2). The model region consists of a circle with a diameter of 32 m. In the center we have a borehole with a diameter of 0.12 m.

The flow field is solved using Darcy´s law.

$$v=\frac{-K}{\rho_W g}\nabla p \tag{1}$$

where v is the Darcy velocity, K the hydraulic conductivity, ρ_W the water density, g the gravitational force and p the pressure.

The outer boundary is defined by a hydraulic head h value which is calculated by using (1) and

$$p=\rho_W g h \ . \tag{2}$$

The inner well boundary is defined by the time-dependent mass flux

$$N_0=\frac{Q(t)}{M\rho_W 2\pi R} \tag{3}$$

where M is the aquifer thickness, R the well radius and $Q(t)$ the time-dependent pumping rate.

The transport of the tracer is modeled using the solute transport mode, respectively the partial differential equation mode.

$$\phi_{eff}\frac{\partial c}{\partial t}-\nabla\left(\left(D_{disp}+D_{diff}\right)\nabla c\right)+v\nabla c=0 \tag{4}$$

with ϕ_{eff} as the eff. porosity, D refers to dispersion/diffusion coefficients and v is the Darcy velocity. c corresponds to the concentration of the normalized tracer. The inner boundary condition is

$$c=1 \tag{5}$$

at the well boundary while injecting and switching to outflow boundary

$$v_x n_x+v_y n_y=0 \tag{6}$$

during shut-in and pumping. The outer boundary is as well an outflow boundary.

The initial condition is

$$c=0 \ . \tag{7}$$

everywhere in the model region.

3.1 Models

The experiment is modeled in three different ways. First we set-up a complete numerical solution by solving the flow field (pressure) with the Darcy´s law (*dl*) and couple this solution with the solute transport mode (*esst*). To save computational power we made two other models which use the analytical solution of the flow field (Table 3). First we apply the *esst* and second we apply the partial differential equation mode (*pde*). The slight difference in computational time between the *esst* model and the *pde* model is that for the *esst* the time-dependent pumping rate is a real step function whereas in the *pde* model the step is transformed into a steep continuous function. This causes a finer resolution at the transfer from one phase of the experiment to the next.

A comparison of the flow-field in the next subsection allows us to use the model with analytical flow field solution.

Table 3: Model statistics and computational time for quadratic shape functions and 8130 elements on an usual desktop pc.

MODEL	*DOF*	*TIME [s]*
dl + esst	32896	277
esst	16448	76
pde	16448	88

The key features of the different models will be described in the following.

dl* and *esst

The flow field is coupled twice to the solute transport mode. First the velocities are directly written into the convection/advection term. Second the dispersion coefficient is velocity depended.

$$D_{xx}=\alpha_l v_x^2+\alpha_t v_y^2/(v)+D_{diff} \tag{8}$$

$$D_{yy}=\alpha_l v_y^2+\alpha_t v_x^2/(v)+D_{diff} \tag{9}$$

$$D_{xy}=D_{yx}=(\alpha_l-\alpha_t)v_x v_y/(v) \tag{10}$$

α_l, α_t are the longitudinal and transversal dispersivities where

$$\alpha_l=10\cdot\alpha_t \tag{11}$$

***esst* and analytical solution**

The model using the solute transport mode is divided into three parts. It starts with the injection phase, followed by the shut-in and the pumping phase. The solution of the preceding step is the starting condition for the next. Therefore we can model sharp steps in the pumping function.

***pde* and analytical solution**

This model is able to solve the hole time-dependent experiment in one run. Therefore we need a boundary condition change from Dirichlet to Neumann within the runtime of the model. While injecting the fluid the well boundary is (5) .

When the injection is finished we change to outflow boundary condition (6).,
This is done by a time-dependent boolean switch in the constraint node of the pde mode.

$$(c-1)\cdot(t<t1)+(v_x n_x+v_y n_y)\cdot(t>t1)=0 \quad (12)$$

Here *t1* is the end of the injection phase.

4. Flow Field

Before we start the main analysis we check the numerical solution against the used analytical solution. Therefore we solve Darcy´s law in the model region. The analytical solution is a superposition of an ambient flow with well flow which comes from an point source and goes in radial direction through a cylindrical plane (Figure 2). While the mass flowing through the plane is conserved the flow velocity decreases with radial distance. One can see marginal deviations between the two solutions due to the circumference of the borehole (Table 4).

$$v_f=\frac{-Q}{2\pi r M}+v_{ambient} \quad (13)$$

This affects the solution on the second digit in the area of interest .

Table 4: First two row correspond to a flow field with ambient flow. Last two rows concern the case without ambient flow.

[m s^{-1}]	*Numerical solution*	*Analytical solution*	*Difference*
V_max	$1.33 \cdot 10^{-4}$	$1.34 \cdot 10^{-4}$	$0.01 \cdot 10^{-4}$
V_min	$1.10 \cdot 10^{-8}$	$1.50 \cdot 10^{-8}$	$0.40 \cdot 10^{-8}$
V_max	$1.33 \cdot 10^{-4}$	$1.33 \cdot 10^{-4}$	$0.00 \cdot 10^{-4}$
V_min	$4.96 \cdot 10^{-7}$	$4.96 \cdot 10^{-7}$	$0.01 \cdot 10^{-7}$

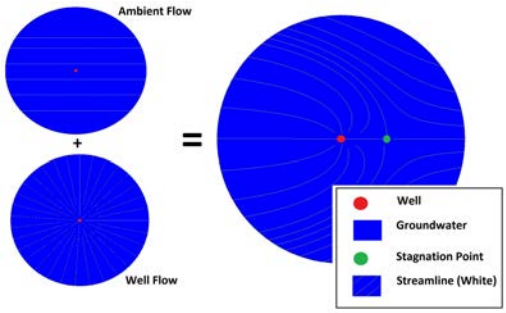

***Figure 2**: Superposition of ambient and well flow field. In dependence of the ambient flow velocity and the pumping rate the scale varies.*

The main result of the experiment is the breakthrough-curve (BTC). This is the measured concentration with respect to time. Since the velocity is changing around the borehole we have to weight the outflowing concentration with the velocity:

$$\bar{c}=\frac{\oint v\cdot c}{\oint v} \quad . \quad (14)$$

5. Experimental Results

The starting model used for the analysis was based on an arbitrary choice. The experiment constraints of the performed tracer test where chosen as well as the reservoir constraints (Tables 1 & 2). As the starting longitudinal dispersivity we take 0.01 m and the ambient flow velocity is 10^{-6} ms^{-1}. For the type curve analysis the injection, quiescence and pumping times are adapted to increase the contrast.

5.1 Sensitivity Analysis

When performing a SWIW there are several parameters known e.g. the duration of the experiment phases, the pumping rates, the concentration and the aquifer thickness. For the interpretation of a BTC there are only a few parameters unknown: porosity, diffusion/dispersion coefficient and ambient groundwater velocity (cf. eq. 4). In the

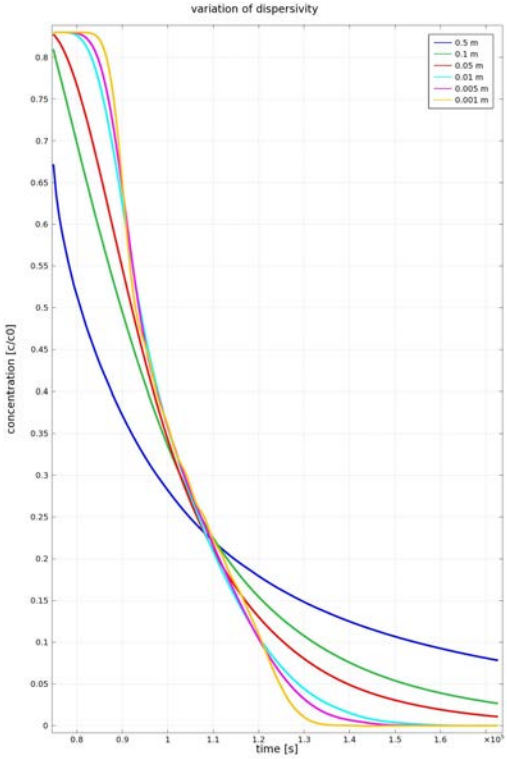

***Figure 3:** The BTC strongly depends on the dispersivity. The variation over a certain range effects the shape of the BTC dramatically. From a step-like BTC for a low dispersivity, over a s-curved shape to a decaying BTC for a rather high dispersivity.*

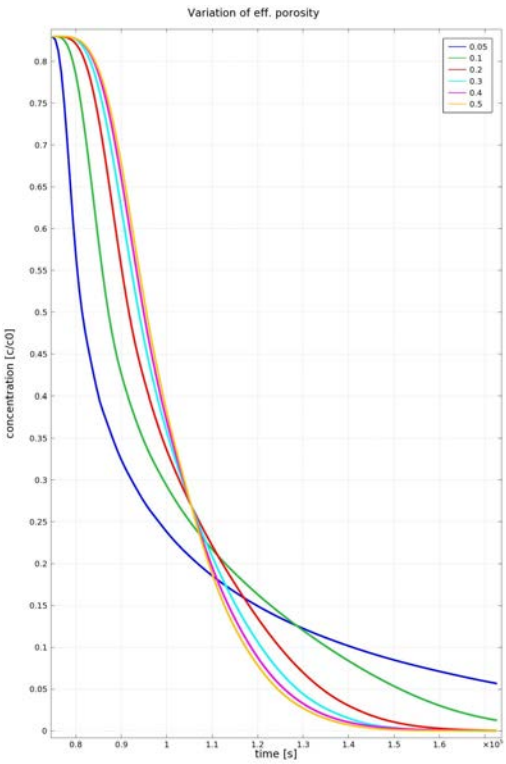

Figure 4: *Variations of the porosity have a minor influence on the BTC. While the principle shape of the BTC is conserved, the porosity changes affect solely the steepness of the BTC. While for a low. porosity the plateau is much longer, we get in contrast longer tailing for a high porosity.*

presents of an ambient flow field the diffusion coefficient can be neglected since it sums up with the dispersion coefficient (cf. eq. 9-10) which is several orders of magnitude higher. The tracer used in this study has only a very low sorption and is chemically stable. So we neglect sorption and reaction processes.

For the sensitivity analysis we have in the first instance a look on effects due to changes dispersivity and porosity.

We choose the dispersivity α_l in a range from 0.001m to 0.5m which correspond to experimental scale up to 10m (Wheatcraft 1988). In Figure 3 one can clearly see a strong dependence of the BTC on the dispersivity. While for small dispersivitys the BTC gets more and more step like with slight deviations due to the ambient flow field. For a high dispersivity the BTC changes its characteristic to a decaying result. This could lead to an ambiguous result which must be considered for further analysis (see below).

In contrast to the potential high impact on the BTC by dispersivity changes the variations of the porosity is less distinct. The general shape of the curve is conserved (Figure 4). The variation of the porosity leads to a change in the flow velocity of the tracer particle which is given by:

$$v_{tracer} = \frac{v}{\phi_{eff}} \tag{17}$$

So for decreasing eff. porosity the tracer travels faster trough the reservoir. Since the dispersion coefficient is velocity depended this causes an impact on the tracer distribution. So we have only in the nearest vicinity of the well the injected concentration and therefore a short plateau. For porosities below 0.03 the results are not valid, since this effective porosity relate to aquiclude or even aquitarde conditions.

5.2 Type Curves for Different Ambient Velocities

The main target of this tracer experiment is the unknown ambient groundwater velocity. To interpret the BTC a parametric study over a wide range of ambient groundwater velocities is conducted. We are able to identify three, respectively four main types.

1. When the tracer remains, due to a very low ambient groundwater velocity, in a more or less radial symmetry around the well we have the s-shaped BTC (Figure 5 upper left picture).
2. When the tracer is between the well and the stagnation point the BTC has in this case an increase of the concentration with an tailing since some amount remains in the slow flowing region around the stagnation point (Figure 5 upper right picture).
3. The third case is the zero line when all the tracer is traveled beyond the stagnation point (Figure 6 upper right picture). In that case the interpretation of the experiment allows only an estimation of the minimum ambient groundwater velocity.

For the interpretation of the BTC we have to take care of the ambiguity due to dispersion effect as shown in Figure 3 a high dipersivity could effect a rather high decay-like decrease of the injected tracer pulse. In that case the type 1 BTC changes to a declining curve which looks similar to the transition from type 1 to type 2 (Figure 5). Type 2 and 3 as well as the transition between these cases is not affected by dispersion changes in terms of curve shape, but it turns out that for high dispersivities the curves flatten out.

The small decrease in the beginning of the BTC is due to numerical artefacts, since the outflow boundary keeps the very value constant when it acts like an inflow boundary.

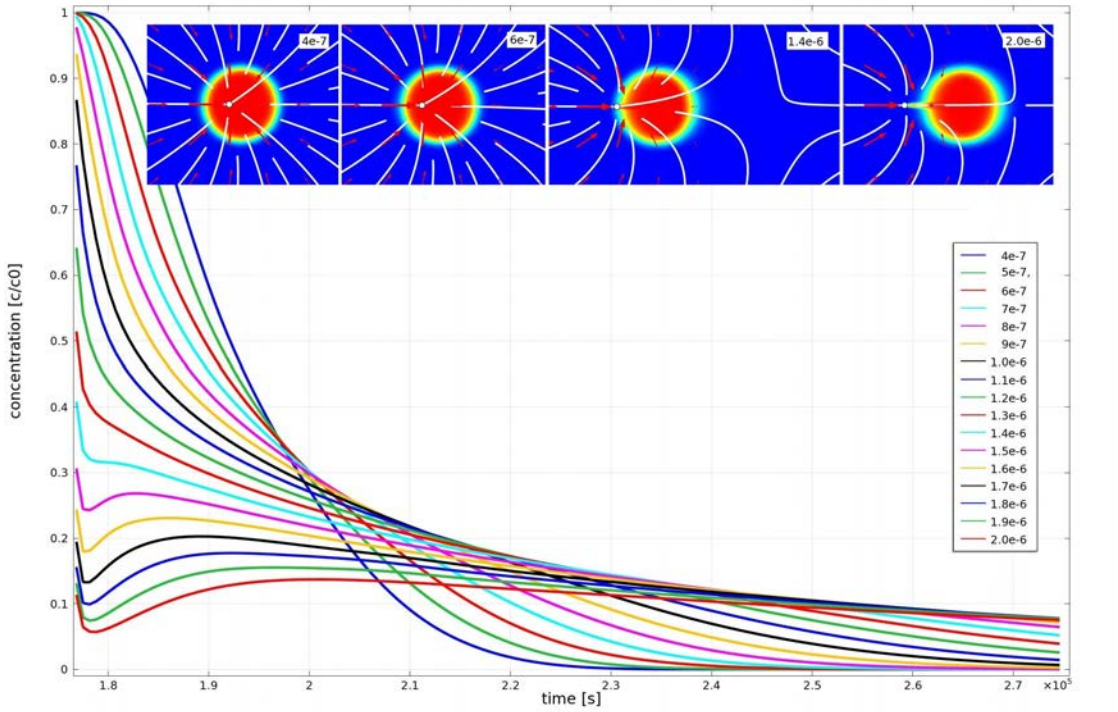

Figure 5: *Upper pictures indicate the tracer distribution in the reservoir at the begin of the pumping phase for different ambient velocities. From flow lines one can clearly see the location of the well and the stagnation point.*

Lower curves show the corresponding BTCs

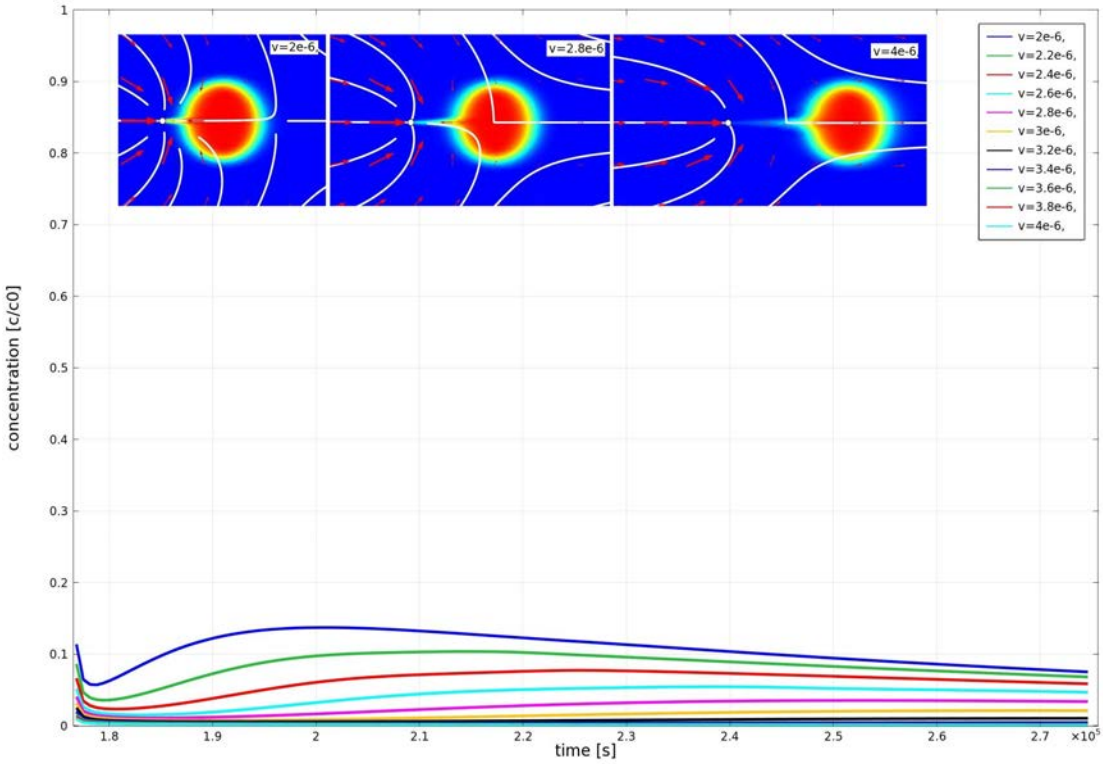

Figure 6: *Upper pictures indicate the tracer distribution in the reservoir at the begin of the pumping phase for different ambient velocities. From flow lines one can clearly see the location of the well and the stagnation point.*

Lower curves show the corresponding BTCs

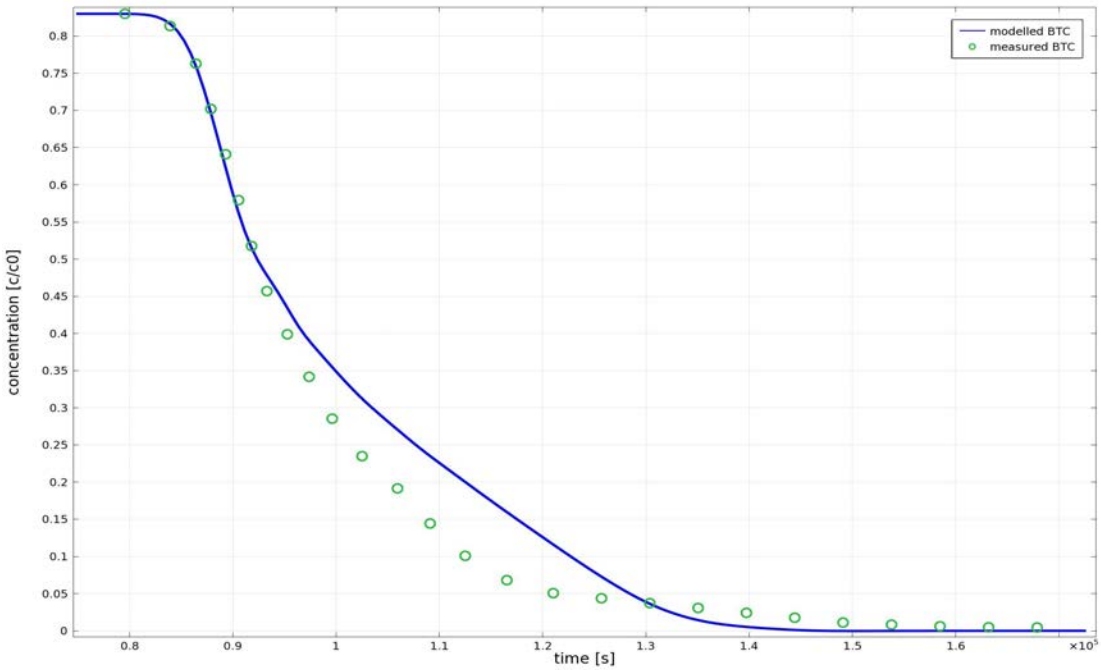

***Figure** 7: Comparison of the modeled BTC to the measured BTC. The curve features are perfectly matched. A plateau at the beginning of the pumping phase, followed by a steep decrease of concentration. Around 0.92 · 10^5 s the decrease flattens in both curves and end with a short tailing.*

6. Discussion and Conclusions

The ability of using a SWIW after Leap and Kaplan (1988) to determine the ambient groundwater velocity is shown. Since there is a very high interaction between well flow and ambient groundwater flow SWIW needs a thorough planing and dimensioning of the length of the experiment phases and the amount of tracer injected.

Comsol Multiphysics provide a powerful tool in estimating the outcome of a SWIW in advance and help interpreting the measured BTC. In this study we are able to interpret the measured BTC with very rough assumptions.

Using the results of the sensitivity analysis and the known eff. porosity from substrate estimates performed by the Technical University Berlin, we are able to interpret the measured BTC (Figure 7) by fitting the dispersivity and ambient groundwater velocity.

The initial drop to 0.83 normalized concentration we relate due to mixing of the tracer fluid with the water column of the well before injection. Since the curve has a plateau this can only occur when the reservoir has a low dispersivity and there is low ambient flow velocity. So the tracer remains in the vicinity of the well. The interpretation of this data must be done very carefully since there are several mechanisms that bias the BTC (Hall 1996). Here we consider a homogenous aquifer with no lateral variations of the hydraulic and reservoir parameters. All special well phenomena like the skin effect etc. are neglected either. Nevertheless a good match of the measured BTC is possible with a longitudinal dispersivity of 0.0025m and an ambient groundwater velocity of $1.1 \cdot 10^{-6}$ ms^{-1}.

The deviations in the second part of the BTC where the decrease of the BTC flattens out could be due to heterogeneity effects since the allocation of the outer rim of the tracer distribution influences the shape of the BTC.

Further studies could focus on the effects of other conceptual flow models like dual porosity flow and fracture flow on the BTC, as well as the consideration of sorbing and reacting tracer.

7. References

1. Leap D. I., Kaplan P.G., A Single-Well Tracing Method for Estimating Regional Advective Velocity in a Confined Aquifer: Theory and Preliminary Laboratory Verification, *Water Resources Research*, **24**, 993-998 (1988)

2. Hall S. H., Practical Single-Well Tracer Methods for Aquifer Testing, *Workshop Notebook, Tenth National Outdoor Action Conference and Exposition*, Las Vegas, Nevada. National Ground Water Association, Columbus, Ohio, USA (1996)
3. Wheatcraft S. W., Scott W. T., An Explanation of Scale-Dependent Dispersivity in Heterogeneous Aquifers Using Concepts of Fractal Geometry, *Water Resources Research*, **24**, 566-578 (1988)

8. Acknowledgements

This work acknowledges financial support from the German Ministry for Environment (BMU) and the EnBW within the project "LOGRO" under grant no. 0325111B, for the opportunity of conducting numerical and field SWIW tracer tests aimed at characterizing deep-sedimentary geothermal reservoirs in Germany. The field data is used by courtesy of Technical University Berlin.